



# Reply to: Is the debate over grana stacking formation finally solved?

Frank Mühl<sup>1</sup>✉, Bart van Oort<sup>2,5</sup>, Sujith Puthiyaveetil<sup>3</sup> and Helmut Kirchhoff<sup>4</sup>✉

REPLYING TO M. M. Gudarzi et al. *Nature Plants* <https://doi.org/10.1038/s41477-021-00880-7> (2021)

In plants, the photosynthetic pigment–protein complexes catalysing energy conversion are harboured in the thylakoid membrane system of chloroplasts. Recent breakthroughs in electron tomography<sup>1–3</sup> reveal the sophisticated architecture of this unique membrane system with stacked grana as a structural hallmark. A long-standing question has been whether the combination of physicochemical forces alone can explain the strict stacking of grana with an inter-membrane separation of 3–4 nm. In our 2017 *Nature Plants* paper<sup>4</sup>, we argued that the balance between attractive van der Waals (vdW) forces ( $F_{\text{vdW}}$ ) and repulsive electrostatic ( $F_{\text{el}}$ ) and hydrostructural ( $F_{\text{hydro}}$ ) forces could explain grana stacking, in contrast with previous reports. Our finding was challenged in the report by Gudarzi et al.<sup>5</sup> This reply addresses this critique.

For estimation of physicochemical stacking forces in grana, the system can be described as two planar (hydrophobic) membranes with embedded proteins separated by an aqueous gap (stromal gap). To calculate vdW forces based on the Hamaker coefficient ( $A$ ), the dielectric permittivities of the membrane ( $\epsilon_{\text{mem}}$ ) and the aqueous stromal gap ( $\epsilon_a$ ) must be known. Since the thylakoid membrane is constituted of a lipid bilayer and transmembrane proteins,  $\epsilon_{\text{mem}}$  is calculated by the volume-weighted permittivities of both,  $\epsilon_p$  (protein) and  $\epsilon_h$  (hydrocarbon lipids). Gudarzi et al. criticized the model we used for  $\epsilon_p$ . Our 2017 paper<sup>4</sup> had indeed updated, based on novel approaches that we introduced, the parameters required for the calculation of physicochemical forces, but we did not update the underlying theory. The theory followed the original work by Sculley et al.<sup>6</sup>, who chose the functional form of  $\epsilon_p$  based on the assumption that it should be similar in shape to that of hydrocarbon phases (see Supplementary Equation 1). This model implies that  $\epsilon_{\text{mem}}$  at visible frequencies is equal to the one at zero frequency<sup>5</sup>. While this assumption is reasonable for the lipid phase, it may be questionable for the protein. Thus, we concur with Gudarzi et al.<sup>5</sup> that  $\epsilon_p$  needs revision.

We took the opportunity for a thorough re-evaluation of vdW forces involved in grana stacking, adopting the form of  $\epsilon_p$  suggested by Gudarzi et al.<sup>5</sup> (see Supplementary Equation 2). It should be noted that this two-oscillator model is still a simplification as it neglects the contribution of protein-bound pigments such as chlorophylls occurring in grana stacks. The influence of these pigments on the dielectric properties of the thylakoid membrane remains to be evaluated. Nonetheless, the optical properties of chlorophylls have been used to estimate the refractive index ( $n$ ) of these proteins, which is required to calculate  $\epsilon_p$ , resulting in  $n = 1.39 \pm 0.04$  (ref. <sup>7</sup>). We used this value in Supplementary Equation 2 together with

$\epsilon_p^{(0)} = 4$ . Note that this choice yields consistently  $\epsilon_p \approx 2$  at  $\xi \approx 2 \text{ eV}$ , which is the absorption maximum of protein-bound chlorophyll *a* (ref. <sup>8</sup>). However,  $\epsilon_p$  should actually exhibit another sigmoidal step in this frequency region. This is why Supplementary Equation 2 remains an approximation.

Our new calculation of the Hamaker coefficient yields  $A = 3.9 \times 10^{-21} \text{ J} = 3.9 \text{ zJ}$  (see Supplementary Information for further details). Considering the uncertainty in the refractive index of the protein, we obtain lower and upper margins of  $2.9 \text{ zJ}$  and  $5.5 \text{ zJ}$ , respectively. These values are indeed significantly smaller than the  $48 \text{ zJ}$  obtained earlier<sup>4</sup>, but overlap with the range of  $4.5$  to  $9.0 \text{ zJ}$  obtained by Gudarzi et al.<sup>5</sup> They also considered retardation effects, which in the range of membrane separation distances between  $2$  and  $8 \text{ nm}$  are, however, not larger than the uncertainties. Thus, in our re-evaluation of the force balance, we neglect retardation and consider three possible values of the Hamaker coefficient  $A$ : (1) our average value of about  $4 \text{ zJ}$ , (2) our maximal value of  $5.5 \text{ zJ}$  and (3) the maximal value of  $9 \text{ zJ}$  suggested by Gudarzi et al.<sup>5</sup> The van der Waals force,  $F_{\text{vdW}}$ , is computed based on the same geometric model as our earlier work<sup>4</sup> (see Supplementary Equation 6).

The second major critique by Gudarzi et al.<sup>5</sup> concerns our determination of the maximum possible surface charge density  $\sigma$  by counting the number of ionizable groups on the stromal membrane surface. This approach assumes a standard protonation state (SPS) for these groups. The SPS is defined as the prevailing protonation state of the isolated group in an aqueous solution at pH 7 (ref. <sup>9</sup>). The  $pK_a$  value of the group, however, can be shifted due to charge–charge interactions with the protein and the influence of the dielectric medium, leading to, for example, an aspartic acid (Asp) side chain to become protonated and, hence, uncharged. This important effect was admittedly not considered in our 2017 paper<sup>4</sup>, but would have been difficult to implement in our method without explicit knowledge of protonation probabilities of surface groups. Coincidentally, such information is meanwhile available from structure-based computations aiming at optical spectra of photosynthetic pigment–protein complexes<sup>9</sup>. Protonation probabilities were computed for a subset of proteins contained in the  $C_2S_2M_2$  supercomplex of *Pisum sativum*<sup>10</sup> (Supplementary Information). These data allow identification of the groups at the stromal surface of the subcomplexes that are likely not in their SPS. A prototypical example is Asp 54 of LHCII (light-harvesting complex II). The Asp residues of the three monomers meet in the centre of the LHCII-trimer, so that their mutual electrostatic interaction causes one of them on average to be protonated at pH 7.5–8.0, a pH range assumed for

<sup>1</sup>Institute for Theoretical Physics, Department of Theoretical Biophysics, Johannes Kepler University Linz, Linz, Austria. <sup>2</sup>Biophysics of Photosynthesis, Department of Physics and Astronomy, Faculty of Science, Vrije Universiteit Amsterdam, Amsterdam, the Netherlands. <sup>3</sup>Department of Biochemistry and Center for Plant Biology, Purdue University, West Lafayette, IN, USA. <sup>4</sup>Institute of Biological Chemistry, Washington State University, Pullman, WA, USA.

<sup>5</sup>Present address: Physical Chemistry and Soft Matter, Wageningen University, Wageningen, the Netherlands. ✉e-mail: [Frank.Mueh@jku.at](mailto:Frank.Mueh@jku.at); [kirchhh@wsu.edu](mailto:kirchhh@wsu.edu)

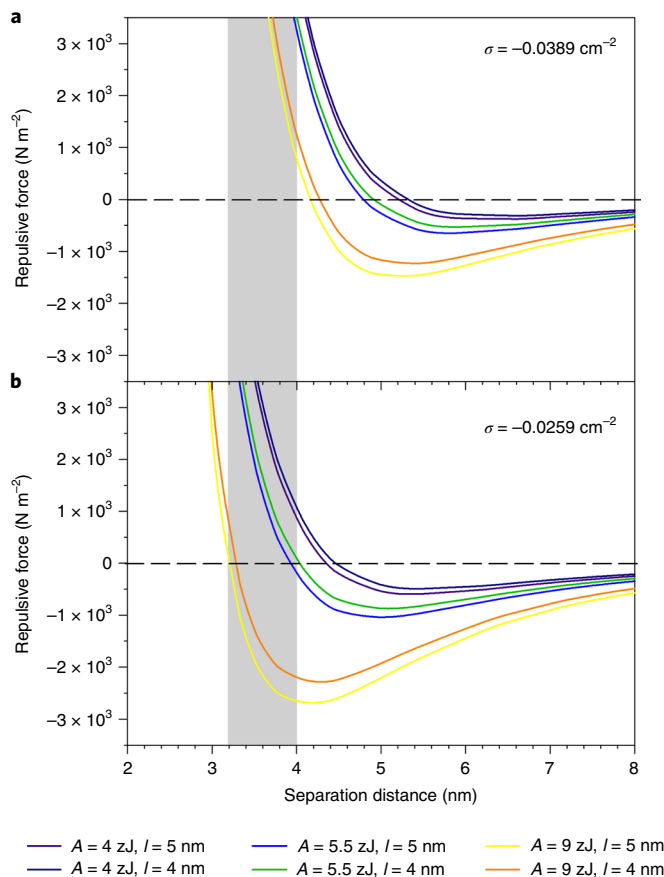


**Fig. 1 | Net repulsive force between granal thylakoid membranes across the stromal gap.** **a,b,** Distance dependence of the sum of all three forces ( $F_{\text{vdW}}$ ,  $F_{\text{el}}$  and  $F_{\text{hydro}}$ ) evaluated for the two different surface charge densities corresponding to standard protonation states (**a**,  $\sigma = -0.0389 \text{ cm}^{-2}$ ) and non-standard protonation states (**b**,  $\sigma = -0.0259 \text{ cm}^{-2}$ ) of titratable groups on the stromal surface of grana-hosted multi-subunit complexes (see Supplementary Information for details) and for different values of the Hamaker coefficient  $A$  and the membrane thickness  $l$ . The grey area indicates the span of measured membrane separation distances. Conditions: 200 mM KCl, 5 mM MgCl<sub>2</sub>,  $T = 293 \text{ K}$ ,  $\epsilon_r = 80$ .

the stroma. As a consequence, we can count one negative charge less per LHCII-trimer. In this way, we re-evaluated the net charges on the stromal side of grana-hosted, multi-subunit complexes (see Supplementary Table 1). Note that this re-evaluation is not exhaustive, since not all complexes could yet be simulated. Nonetheless, the data give a first estimate of the decrease in the magnitude of the surface charge density due to  $pK_a$  shifts of protein-bound groups. The effect is indeed significant: the surface charge density is changed from  $\sigma = -0.0389 \text{ cm}^{-2}$  in the SPS (no phosphorylation) to  $\sigma = -0.0259 \text{ cm}^{-2}$  for the non-standard protonation states (Supplementary Table 2). We recalculated the repulsive electrostatic force  $F_{\text{el}}$  using a refined numerical algorithm (see Supplementary Information for details).

The net force between the thylakoid membranes across the stromal gap is given by  $F = F_{\text{vdW}} + F_{\text{el}} + F_{\text{hydro}}$ , where the hydrostructural force is calculated according to  $F_{\text{hydro}} = 10^{10} e^{-d/0.193} \text{ Nm}^{-2}$ , as before<sup>4</sup>. Figure 1 shows the net force at 200 mM KCl and 5 mM MgCl<sub>2</sub> in the stromal gap as a function of the membrane separation distance. It is noteworthy that even with the smaller Hamaker coefficients, force balance (zero crossing) can be achieved for the original surface charge density without protein phosphorylation<sup>4</sup> (Fig. 1a),

but the membrane separation distances are between 4.2 and 5.3 nm, that is, somewhat larger than the experimentally determined range of  $3.6 \pm 0.4 \text{ nm}$ <sup>11</sup>. Decrease in the magnitude of the surface charge density due to non-standard protonation states shifts the equilibrium distances right into the range of experimental values (Fig. 1b). Experiments suggest a membrane thickness of  $4.0 \pm 0.2 \text{ nm}$ <sup>11</sup>. Using  $l = 4 \text{ nm}$  in Supplementary Equation 6, the experimental membrane separation distances can be reproduced with Hamaker coefficients between 5.5 and 9.0 zJ (Fig. 1b).

The good agreement between measured and computed equilibrium distance requires high electrolyte concentrations. Decreasing the KCl concentration to 100 mM shifts the distance to values  $\geq 6 \text{ nm}$ . A reduction of the MgCl<sub>2</sub> concentration from 5 mM to 1 mM (at 200 mM KCl) results in a moderate increase of the membrane distance from 3.2–4.4 nm to 3.5–4.8 nm (data not shown). In agreement with our earlier data, no stable intermembrane distance within 8 nm could be observed for a KCl concentration of 20 mM. Thus, our results suggest that the K<sup>+</sup> activity in the stroma is close to the upper limit of values reported in the literature<sup>4</sup>. However, this conclusion is tentative as we neglect binding of ions to the membrane surface in our computations, an issue also raised by Gudarzi et al.<sup>5</sup> Cation binding to the membrane could further reduce the negative surface charge density, so that shorter equilibrium distances could possibly be obtained with lower electrolyte concentrations.

In summary, we confirm the conclusion of our 2017 paper<sup>4</sup>, that the grana stacking can principally be understood based on the force balance between  $F_{\text{vdW}}$ ,  $F_{\text{el}}$  and  $F_{\text{hydro}}$ , although key parameters had to be revised. In particular, a physically realistic modelling of the protein permittivity and a reduction of the surface charge density due to protonation equilibria turned out to be crucial for the theory to work. However, we also conclude that the theory of grana formation may require further refinement.

Received: 5 August 2020; Accepted: 11 February 2021;  
Published online: 11 March 2021

## References

1. Bussi, Y. et al. Fundamental helical geometry consolidates the plant photosynthetic membrane. *Proc. Natl Acad. Sci. USA* **116**, 22366–22375 (2019).
2. Daum, B., Nicastro, D., Il, J. A., McIntosh, J. R. & Kühlbrandt, W. Arrangement of Photosystem II and ATP synthase in chloroplast membranes of spinach and pea. *Plant Cell* **22**, 1299–1312 (2010).
3. Austin, J. R. & Staehelin, L. A. Three-dimensional architecture of grana and stroma thylakoids of higher plants as determined by electron tomography. *Plant Physiol.* **155**, 1601–1611 (2011).
4. Puthiyaveetil, S., van Oort, B. & Kirchhoff, H. Surface charge dynamics in photosynthetic membranes and the structural consequences. *Nat. Plants* **3**, 17020 (2017).
5. Gudarzi, M. M., Aboutalebi, S. H. & Satalov, A. Is the debate over grana stacking formation finally solved? *Nat. Plants* <https://doi.org/10.1038/s41477-021-00880-7> (2021).
6. Sculley, M. J., Duniec, J. T., Thorne, S. W., Chow, W. S. & Boardman, N. K. The stacking of chloroplast thylakoids: quantitative analysis of the balance of forces between thylakoid membranes of chloroplasts, and the role of divalent cations. *Arch. Biochem. Biophys.* **201**, 339–346 (1980).
7. Renger, T. et al. Thermally activated superradiance and intersystem crossing in the water-soluble chlorophyll binding protein. *J. Phys. Chem. B* **113**, 9948–9957 (2009).
8. Mühl, F. & Zouni, A. Extinction coefficients and critical solubilisation concentrations of photosystems I and II from *Thermosynechococcus elongatus*. *Biochim. Biophys. Acta* **1708**, 219–228 (2005).
9. Renger, T. & Mühl, F. Understanding photosynthetic light-harvesting: a bottom up theoretical approach. *Phys. Chem. Chem. Phys.* **15**, 3348–3371 (2013).
10. Su, X. et al. Structure and assembly mechanism of plant C<sub>2</sub>S<sub>2</sub>M<sub>2</sub>-type PSII–LHCII supercomplex. *Science* **357**, 815–820 (2017).
11. Kirchhoff, H. et al. Dynamic control of protein diffusion within the granal thylakoid lumen. *Proc. Natl Acad. Sci. USA* **108**, 20248–20253 (2011).

## Acknowledgements

This work was supported by grants to H.K. from the National Science Foundation (NSF-MCB-1616982 and 1953570), the US Department of Energy (DE-SC 0017160) and the US Department of Agriculture (ARC grant WNP00775), to S.P. from DOE (DE-SC0020639) and USDA-NIFA (Hatch: 1013608) as well as to F.M. by the Austrian Science Fund (FWF) in conjunction with the district of Upper Austria (P 33154-B and P 33155-NBL) and the Linz Institute of Technology (LIT-2019-8-SEE-120). B.v.O. was supported by the Novo Nordisk Foundation project 'Harnessing the Energy of the Sun for Biomass Conversion' (NNF16OC0021832).

## Author contributions

F.M. and H.K. performed calculations. F.M., B.v.O., S.P. and H.K. designed the study and wrote the manuscript.

## Competing interests

The authors declare no competing interests.

## Additional information

**Supplementary information** The online version contains supplementary material available at <https://doi.org/10.1038/s41477-021-00881-6>.

**Correspondence and requests for materials** should be addressed to F.M. or H.K.

**Reprints and permissions information** is available at [www.nature.com/reprints](http://www.nature.com/reprints).

**Publisher's note** Springer Nature remains neutral with regard to jurisdictional claims in published maps and institutional affiliations.

© The Author(s), under exclusive licence to Springer Nature Limited 2021